The Oncologist®

Neuro-Oncology

Defining Treatment-Related Adverse Effects in Patients with Glioma: Distinctive Features of Pseudoprogression and Treatment-Induced Necrosis

Sebastian F. Winter,[a,b,f,g] Eugene J. Vaios,[a] Alona Muzikansky,[c] Maria Martinez-Lage,[d] Marc R. Bussière,[e] Helen A. Shih,[e] Jay Loeffler,[e] Philipp Karschnia,[a,h] Franziska Loebel,[f,g] Peter Vajkoczy,[f,g] Jorg Dietrich[a,b]

[a]Massachusetts General Hospital Cancer Center, [b]Department of Neurology, [c]Biostatistics Center, [d]CS Kubik Laboratory for Neuropathology, and [e]Department of Radiation Oncology, Massachusetts General Hospital and Harvard Medical School, Boston, Massachusetts, USA; [f]Department of Neurosurgery, Charité – Universitätsmedizin Berlin, corporate member of Freie Universität Berlin, Humboldt-Universität zu Berlin, Berlin, Germany; [g]Berlin Institute of Health, Berlin, Germany; [h]Department of Neurosurgery, Ludwig Maximilians University, Munich, Germany

Disclosures of potential conflicts of interest may be found at the end of this article.

Key Words. Tissue necrosis • Pseudoprogression • Treatment-related effects • Malignant glioma • Neurotoxicity

Abstract

Background. Pseudoprogression (PP) and treatment-induced brain tissue necrosis (TN) are challenging cancer treatment–related effects. Both phenomena remain insufficiently defined; differentiation from recurrent disease frequently necessitates tissue biopsy. We here characterize distinctive features of PP and TN to facilitate noninvasive diagnosis and clinical management.

Materials and Methods. Patients with glioma and confirmed PP (defined as appearance <5 months after radiotherapy [RT] completion) or TN (>5 months after RT) were retrospectively compared using clinical, radiographic, and histopathological data. Each imaging event/lesion (region of interest [ROI]) diagnosed as PP or TN was longitudinally evaluated by serial imaging.

Results. We identified 64 cases of mostly (80%) biopsy-confirmed PP (n = 27) and TN (n = 37), comprising 137 ROIs in total. Median time of onset for PP and TN was 1 and 11 months after RT, respectively. Clinically, PP occurred more frequently during active antineoplastic treatment, necessitated more steroid-based interventions, and was associated with glioblastoma (81 vs. 40%), fewer *IDH1* mutations, and shorter median overall survival. Radiographically, TN lesions often initially manifested periventricularly (n = 22/37; 60%), were more numerous (median, 2 vs. 1 ROIs), and contained fewer malignant elements upon biopsy. By contrast, PP predominantly developed around the tumor resection cavity as a non-nodular, ring-like enhancing structure. Both PP and TN lesions almost exclusively developed in the main prior radiation field. Presence of either condition appeared to be associated with above-average overall survival.

Conclusion. PP and TN occur in clinically distinct patient populations and exhibit differences in spatial radiographic pattern. Increased familiarity with both conditions and their unique features will improve patient management and may avoid unnecessary surgical procedures. ***The Oncologist*** 2020;25:e1221–e1232

Implications for Practice: Pseudoprogression (PP) and treatment-induced brain tissue necrosis (TN) are challenging treatment-related effects mimicking tumor progression in patients with brain cancer. Affected patients frequently require surgery to guide management. PP and TN remain arbitrarily defined and insufficiently characterized. Lack of clear diagnostic criteria compromises treatment and may adversely affect outcome interpretation in clinical trials. The present findings in a cohort of patients with glioma with PP/TN suggest that both phenomena exhibit unique clinical and imaging characteristics, manifest in different patient populations, and should be classified as distinct clinical conditions. Increased familiarity with

Correspondence: Sebastian F. Winter, B.Sc., Department of Neurosurgery, Charité – Universitätsmedizin Berlin, Charitéplatz 1, 10117 Berlin, Germany. Telephone: 49-17672807577; e-mail: sebastian-friedrich.winter@charite.de, sfwinter@mgh.harvard.edu; or Jorg Dietrich, M.D., Ph.D., Department of Neurology and Massachusetts General Hospital Cancer Center, Massachusetts General Hospital, Harvard Medical School, 55 Fruit St., Yawkey 9E, Boston, Massachusetts 02114, USA. Telephone: 617-643-6593; e-mail: Dietrich.Jorg@mgh.harvard.edu Received February 4, 2020; accepted for publication April 27, 2020; published Online First on June 18, 2020. http://dx.doi.org/10.1634/theoncologist.2020-0085

PP and TN key features may guide clinicians toward timely noninvasive diagnosis, circumvent potentially unnecessary surgical procedures, and improve response assessment in neuro-oncology.

Introduction

Cancer treatment–related adverse effects on the brain are a major diagnostic and therapeutic challenge in neuro-oncology [1–3]. Pseudoprogression (PP) [4] and treatment-induced brain tissue necrosis (TN) [1] remain insufficiently characterized conditions increasingly encountered in patients with malignant glioma after standard-of-care chemoradiation (chemo-RT) treatment [4, 5]. Because PP and TN are frequently indistinguishable from recurrent disease on conventional imaging [6–9], many patients require tissue biopsy to guide further management, resulting in potentially unnecessary surgical interventions in a significant number of patients. Moreover, patients with treatment-related changes misclassified as progressive disease present a major challenge for appropriate clinical trial enrollment and can adversely affect outcome interpretation, especially in cases that manifest >12 weeks after radiotherapy (RT), that is, beyond the cutoff point currently stipulated in the Response Assessment in Neuro-Oncology (RANO) criteria [1, 10].

The pathology of PP and TN remains incompletely understood [11]. PP likely represents a unique clinical scenario encountered in patients with high-grade gliomas (HGGs; World Health Organization [WHO] grades III–IV) within the first few months of chemo-RT initiation [4, 12–14]. Conversely, TN commonly occurs 6 months to several years—sometimes up to a decade—after initiation of (chemo-)RT, may be irreversible and progressive, and can be associated with significant patient morbidity and mortality [1, 2, 5, 15, 16]. As both conditions are primarily distinguished based on their temporal manifestation, they are often arbitrarily defined and used interchangeably in the literature [17]. Reports of "early necrosis" (TN onset <5 months from RT completion) after temozolomide (TMZ)-based chemo-RT add further diagnostic ambiguity to this classification system in the absence of biopsy-proven features to accurately guide clinical diagnosis and management [18, 19]. Because histopathological criteria specific to each condition have not been established, histopathological findings are commonly summarized as "treatment effect." Efforts to improve noninvasive differentiation of both conditions from recurrent disease have focused on advanced functional imaging [20, 21]. Although positron emission tomography (PET) with novel amino acid tracers (e.g., fluoro-ethyl-tyrosine–PET), computed tomography perfusion studies, multivoxel magnetic resonance (MR) spectroscopy, and combined MR-PET have shown promise in augmenting diagnostic certainty, tissue biopsy remains the diagnostic gold standard [1, 11, 20]. Symptoms associated with PP and TN are commonly managed with steroids or surgical resection [4]. In addition, bevacizumab, anticoagulant drugs, and hyperbaric oxygen therapy have shown some benefit in select patients [1, 5]. Progress in the field has been limited because of a paucity of biopsy-controlled studies, the lack of high-powered prospective randomized controlled trials, and poor standardization across diagnostic imaging modalities used in studies [20, 22]. We here aim to characterize the key clinical and imaging features of PP and TN in patients with malignant glioma in an attempt to improve the current understanding of these conditions, facilitate noninvasive diagnosis of treatment-related adverse effects, and improve response assessment in neuro-oncology.

Materials and Methods

We conducted a retrospective analysis of demographic, clinical, radiographic, and histopathological data from 60 patients with brain tumors diagnosed with PP or TN after glioma therapy at the Massachusetts General Hospital (MGH) between 1997 and 2015. Patient data were obtained from an MGH institutional database. This study received institutional review board approval for all activities.

Eligibility

All 60 patients were treated at MGH and met the following eligibility criteria: (a) tissue-based diagnosis of glioma (WHO grades I–IV) between December 1997 and November 2015, (b) antineoplastic treatment (radiation with or without chemotherapy), and (c) biopsy-proven or clinico-radiographically established diagnosis of treatment-related effects based on serial imaging.

Classification of Treatment Effects

Individual treatment-related effects were primarily characterized based on the time of radiographic appearance of each lesion (hereinafter referred to as region of interest [ROI]) after RT. ROI appearance <5 months after completion of RT was defined as PP, whereas appearance ≥5 months was defined as TN, based on current consensus [1, 2, 5, 15, 16]. For comparative statistical analysis, patients were categorized accordingly and allocated to either PP or TN groups. Notably, 2 of 60 patients presented with lesions classified as "early TN" before the 5-month cutoff [18, 19]. Moreover, 4 of 60 patients presented with both biopsy-proven early PP and later TN and were therefore included in both groups. Accordingly, a total of 64 cases of treatment-related effects were identified and analyzed this cohort of 60 patients.

Variables

We collected demographic, clinical, therapeutic, and outcome parameters for each patient. Variables specific to the initial manifestation of treatment-related effects (first ROI) included characteristics of radiographic onset (time interval from RT completion; onset during active therapy vs. during surveillance), presence of new neurologic symptoms, type of treatment for PP/TN (if any), advanced diagnostic imaging results (if any), histopathological features (if biopsied), and overall number of ROIs developed throughout the condition.

Variables of interest collected for each individual ROI included time of onset after RT completion, duration until complete radiographic resolution (whenever traceable), anatomical aspects (lobar vs. deep-seated [corpus callosum, cingulate gyrus, basal ganglia, thalamus, brainstem,

Table 1. Summary of patient characteristics, treatment specifics, and clinical outcome

Patient characteristics	Total cohort	PP group	TN group	*p* value[a]
Demographics				
Sex ratio (m/f), %	56/44	67/33	49/51	.29456
Median age at diagnosis, years	53	55	47	.08752
Tumor specifics				
Tumor burden, %				.33091
Single lesion	75	67	81	
Multifocal disease	25	33	19	
Intercranial location, %				.05799
Left	42	59	30	
Central	50	41	57	
Mixed	8	0	13	
WHO grade, % (*n*)				.02750
I	1.5 (1)	0 (0)	2.7 (1)	
II	10.9 (7)	0 (0)	18.9 (7)	
III	29.7 (19)	18.5 (5)	37.8 (14)	
IV	57.8 (37)	81.5 (22)	40.5 (15)	
Molecular-genetic profile, % (*n*)				
IDH1 mutated	41.5 (17/41)	11.1 (2/18)	65.2 (15/23)	.00548
MGMT methylated	58.8 (20/34)	52.6 (10/19)	66.6 (10/15)	.61115
Clinical status, %				
With cardiovascular comorbidities	64.1	70.4	59.5	.56611
Earliest KPS (median) after initial surgery	90	90	90	.87992
Treatment specifics				
Extent of surgical resection, *n*				.64589
GTR	18	8	10	
NTR	11	6	5	
STR	20	9	11	
PR	6	4	2	
Biopsy only	5	0	5	
Regimen				
Proton/photon RT, *n*	5/59	1/26	4/33	—
With (modified) TMZ-based standard chemo-RT, % (*n*)	68.8	88.9	54.1	.01534
With concurrent Ctx, % (*n*)	76.6	92.6	64.9	.04579
Steroid use, % (*n*)	70.1 (44/62)	81.5 (22/27)	62.9 (22/35)	.24848
Bevacizumab use, % (*n*)	58.1 (36/62)	63 (17/27)	54.3 (19/35)	.67511
Clinical outcome				
OS, median (95% CI), years	6.25 (0.94–11.56)	3.0 (2.08–3.92)	Not reached[b]	<.0001
With recurrence, % (*n*)	59.6 (34/57)	83.3 (20/24)	42.4 (14/33)	.03062

[a]For difference between groups; false discovery rate–adjusted for multiple hypothesis testing.
[b]Last observation censored at 24.9 years (OS estimate at 62%).
Abbreviations: chemo-RT, chemoradiation; CI, confidence interval; Ctx, chemotherapy; f, female; GTR, gross-total resection; KPS, Karnofsky performance status; m, male; NTR, near-total resection; OS, overall survival; PP, pseudoprogression; PR, partial resection; RT, radiotherapy; TMZ, temozolomide; TN, treatment-induced brain tissue necrosis; STR, subtotal resection; WHO, World Health Organization.

cerebellum, and all periventricular locations] location; periventricular involvement; non-nodular enhancement within or around the resection cavity margins), maximum size, shortest distance from the tumor resection cavity margin, degree of radiation dose exposure, and histopathological characteristics (distinction between pure treatment effect, treatment effect with rare atypical cells, or mostly treatment effect mixed with foci of solid tumor).

Radiographic Analysis

Radiographic analysis of T1-weighted gadolinium enhanced MR imaging (MRI) sequences was carried out with each

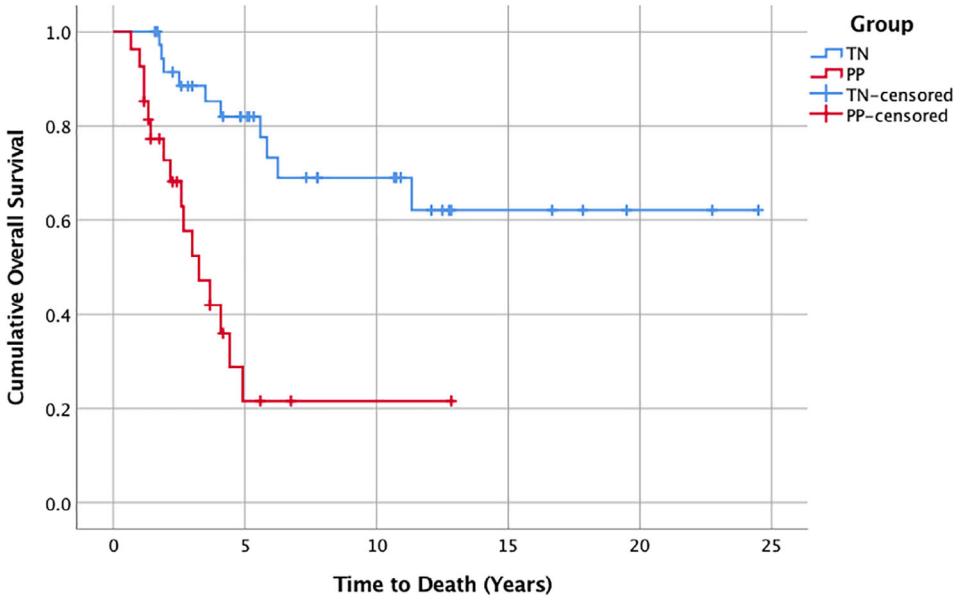

Figure 1. Kaplan-Meier survival analysis depicting PP and TN groups. PP group (red line): 16 progression events; 11 censored. Median overall survival was 3.25 years (95% confidence interval, 2.16–4.9). TN group (blue line): 10 progression events; 27 censored. Median overall survival was not reached. Last observation was censored at 24.5 years, with an overall survival estimate of 62%. For comparison, $p < .0001$.
Abbreviations: PP, pseudoprogression; TN, treatment-induced brain tissue necrosis.

patient using standard clinical imaging software. The date of appearance of diagnosed treatment-related effects was determined retrospectively and defined as the date of the first MRI demonstrating de novo contrast enhancement (T1-gadolinium sequence) in the respective anatomical location of the ROI.

Depending on sufficient availability of follow-up MRI scans, the spatiotemporal pattern of each ROI was traced longitudinally over time. Radiographic measurements of ROI area were carried out for each available MRI scan. ROIs displaying a non-nodular, circumferential enhancement pattern around the tumor resection cavity margin were excluded from size measurements.

The radiographic duration of treatment-related effects was defined for each ROI as the time of first radiographic appearance on MRI until complete radiographic resolution or last available MRI. Reasons for discontinuation of measurements included treatment (surgical resection of ROI or systemic treatment with bevacizumab) or tumor recurrence at the same ROI. The shortest ROI-to-resection cavity margin distance (mm) was measured in axial, coronal, or sagittal planes using the MRI of first radiographic appearance for each ROI. Whenever available, the patient's RT dose distribution was correlated to the anatomical location of each ROI as a proxy for the extent of radiation dose exposure (below, at, or above maximal therapeutic target value; in Gy) received. Diagnostic results from MR perfusion (MRP) and diffusion weighted imaging (DWI) studies, if available, were interpreted with respect to the patients' ROIs and included in the analysis.

Statistical Analysis

Descriptive statistics were used to analyze clinical and radiographic features for both groups. For associations between groups, p values were determined using chi-square and Fisher's exact tests for categorical variables and a Wilcoxon rank-sum test for continuous variables. All reported p values were adjusted for multiple hypothesis testing by false discovery rate; statistical significance was considered as $p < .05$. The Kaplan-Meier (KM) method was used to calculate median overall survival (OS); median follow-up time was calculated based on the reverse KM estimator approach.

In order to statistically compare radiographic and histopathological features of individual ROIs between patient groups, a logistic regression analysis using a univariate generalized estimating equation (GEE) model, predicting affiliation with TN group as the function of the tested variable and adjusting for repeated observations within a patient, was used. GEE-based analysis was purposefully limited to eight preselected variables of interest and statistical significance was reported using p values and parameter estimates for directionality.

Results

A total of 64 cases of treatment-related effects, classified as either PP ($n = 27$) or TN ($n = 37$), were identified and analyzed. Diagnosis of treatment-related effects was mostly secured by tissue biopsy; the remainder of cases (20%) were confirmed through longitudinal clinico-radiographic follow-up. All patients had previously undergone RT (most with concurrent and sequential chemotherapy), predominantly for HGG diagnosis (87.5%). Baseline patient performance status at time of diagnosis was generally high (median Karnofsky performance status [KPS] after initial surgery, 90/100); cardiovascular comorbidities were present in almost two-thirds of patients. Incidence of recurrence was 60%, and median

Table 2. Characteristics of first ROI identified as treatment effect

Characteristics of first ROI	Total cohort	PP group	TN group	*p* value[a]
Spatiotemporal radiographic features				
Onset after RT completion, median (range), months	6.5 (0–239)	1.0 (0–4)	11.0 (3–239)	<.00001
Periventricular location, %	48.4	33.3	59.5	.09098
Ring-like enhancement around RC, %	37.5	70.4	13.5	.00009
Functional imaging features, % (*n*)				
With functional imaging	77.4 (48/62)	92.0 (23/25)	67.6 (25/37)	.07587
Elevated rCBV in MRP	75.0 (30/40)	88.8 (16/18)	63.6 (14/22)	.19976
Restricted diffusion in DWI	54.1 (20/37)	57.7 (8/14)	52.2 (12/23)	.75603
Clinical features				
Onset during active treatment, %	54.7	85.2	32.4	.00044
Amount of Ctx received prior to onset, median (IQR), months	3.0 (1–9)	1.0 (1–3)	7.5 (2–12)	.00574
With concurrent new symptoms, % (*n*)	65.6 (40/61)	69.2 (18/26)	62.9 (22/35)	.82835
Symptoms related to ROI, % (*n*)	60.0 (24/40)	59.1 (13/22)	61.1 (11/18)	.61115
Receiving any treatment for ROI, %	78.1	88.9	70.2	.20967
Receiving steroids, %	54.7	74.1	40.5	.03592
Receiving bevacizumab, %	18.8	11.1	24.3	.29698
Receiving surgical debulking, %	35.9	51.9	24.3	.07991
Histopathological features, % (*n*)				.03592
Treatment effect only	16.0 (8/50)	0.0 (0/24)	30.8 (8/26)	
Treatment effect with rare atypical cells	62.0 (31/50)	70.8 (17/24)	53.8 (14/26)	
Treatment effect with foci of solid tumor	22.0 (11/50)	29.2 (7/24)	15.4 (4/26)	

[a]For difference between groups; false discovery rate–adjusted for multiple hypothesis testing.
Abbreviations: Ctx, chemotherapy; DWI, diffusion weighted imaging; IQR, interquartile range; MRP, magnetic resonance perfusion; PP, pseudoprogression; RC, resection cavity; rCBV, relative cerebral blood volume; ROI, region of interest; RT, radiotherapy; TN, treatment-induced brain tissue necrosis.

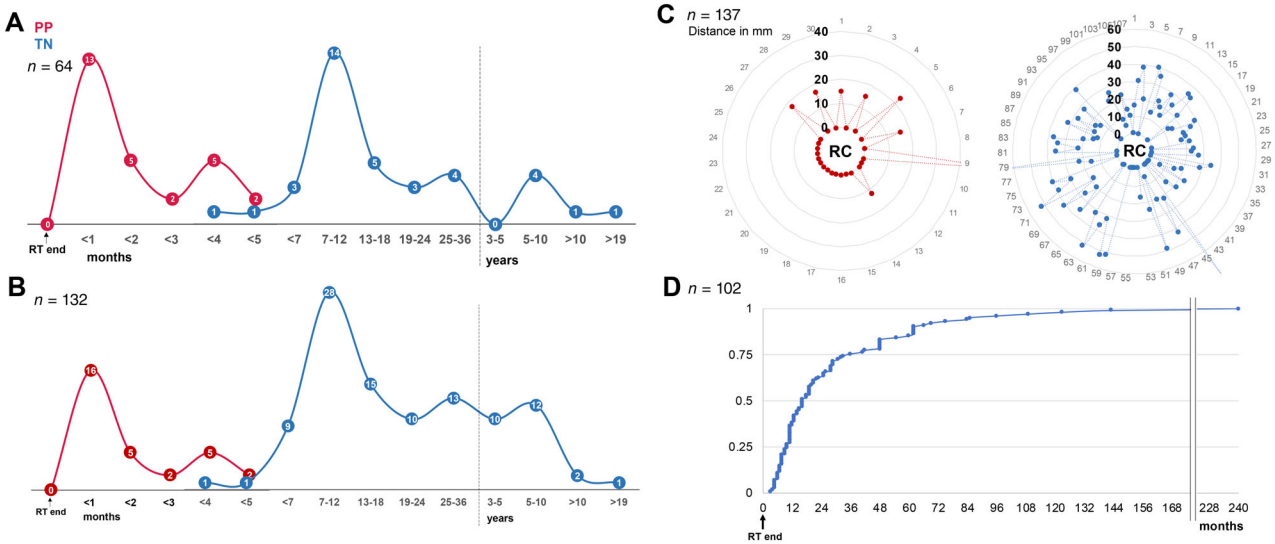

Figure 2. Spatiotemporal radiographic pattern of PP and TN lesions. **(A):** Temporal distribution of first region of interest (ROI) manifestation on magnetic resonance imaging (MRI) after RT completion. **(B):** Temporal distribution of overall ROI manifestation on MRI after RT completion. **(C):** Spatial distribution of ROIs relative to the tumor resection cavity (RC), illustrating shortest ROI-to-RC distances for each ROI. **(D):** Cumulative frequency of TN group ROI onset latency from RT completion.
Abbreviations: PP, pseudoprogression; RT, radiotherapy; TN, treatment-induced brain tissue necrosis.

OS was 6.25 (95% confidence interval, 0.94–11.56) years (Table 1). To characterize putative differences in clinical and spatiotemporal radiographic features between both types of treatment-related effects, an in-depth comparative analysis between patients with PP versus those with TN was carried out.

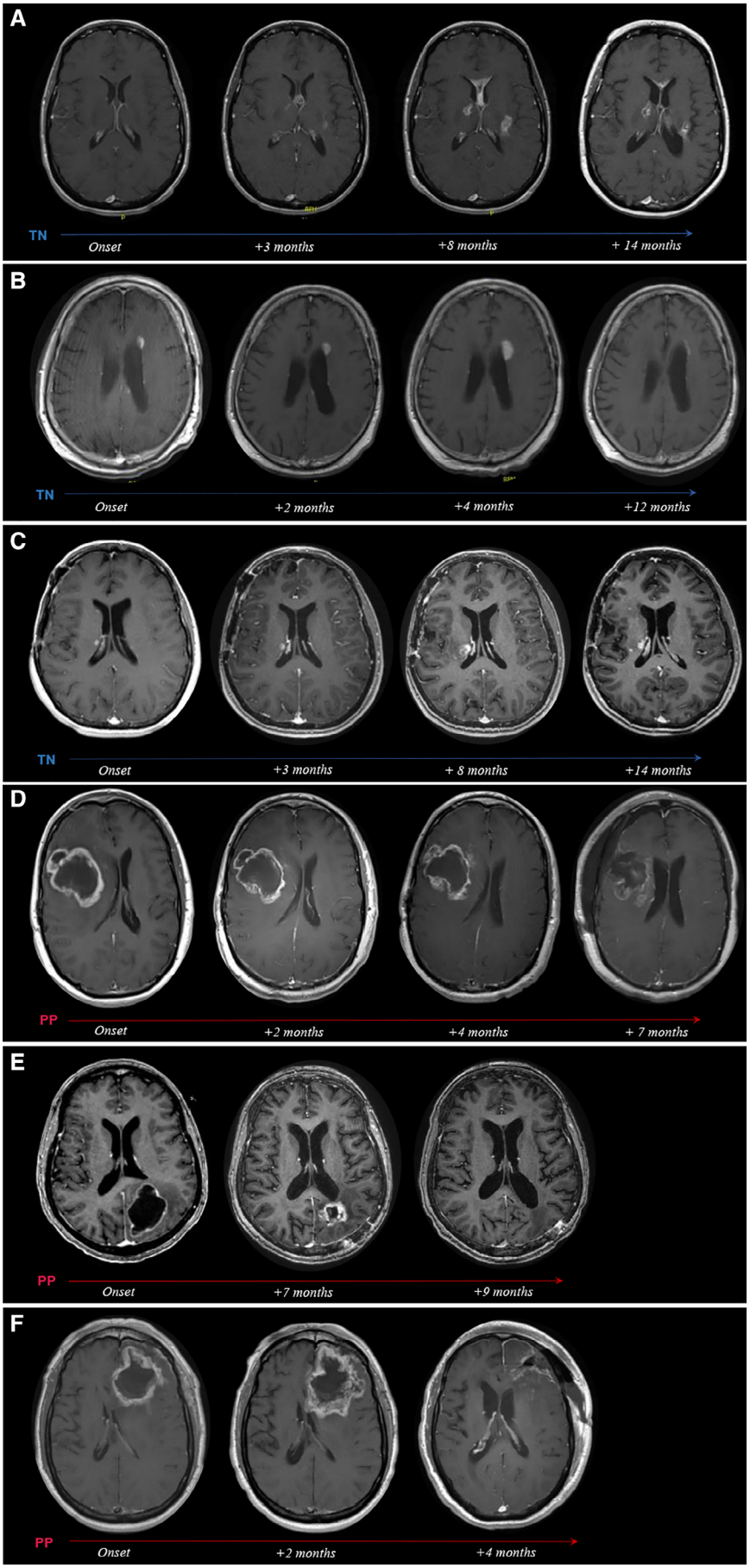

Differences in Patient Characteristics, Treatment Specifics, and Clinical Outcome

Age, gender, and KPS did not significantly differ between patients with PP and TN, although the former group was older (median age at time of diagnosis, 55 vs. 47 years) and had a slightly higher incidence of cardiovascular comorbidities (70.4 vs. 59.5%). The PP group had a significantly larger proportion of glioblastoma cases (81.5 vs. 40.5%; $p < .002$), with a higher fraction of tumors localized to left cerebral hemispheres that trended toward significance (59 vs. 30%; $p = .058$). Analysis of associated tumor molecular-genetic profiles in this group revealed considerably fewer *IDH1* mutations (11.1 vs. 65.2%; $p < .006$) and a slightly lower incidence of *MGMT* promoter methylation (52.6 vs. 66.6%), as compared with the TN group (Table 1).

Most cases in both groups were treated with open surgical resection followed by standard chemo-RT treatment. In line with the high incidence of glioblastoma multiforme (GBM; 81.5%) observed in patients with PP, concurrent chemotherapy ($p < .05$) and TMZ-based standard chemo-RT regimens ($p = .015$) were more frequently administered in this group. In addition, steroid-based interventions and bevacizumab use were slightly more pronounced. Median follow-up times for PP and TN groups were 5.6 and 10.7 years, respectively. Compared with the TN group, the rate of disease recurrence in patients with PP was nearly twice as high ($p = .03$; Table 1). The median OS on Kaplan-Meier survival analysis was 3.25 years for patients with PP. Patients in the TN group survived substantially longer (median OS not reached; 62% survival estimate, last observation censored at 24.5 years; $p < .0001$; Fig. 1). The 5-year survival rates for PP and TN groups were 26% and 82%, respectively.

Differences in Initial Clinico-Radiographic Presentation

Analysis of both spatiotemporal radiographic pattern and biopsy features of patients' first appearing lesion ("first ROI") revealed significant differences between PP and TN groups (Table 2).

Although group allocation per se was based on temporal stratification (5-month cutoff point), both PP and TN were found to exhibit specific temporal incidence peaks. As such, most PP lesions developed within weeks after RT completion (median onset, 1 month), thus more often manifesting during active antineoplastic treatment (85 vs. 32%; $p < .0005$). Conversely, TN incidence peaked between 7 and 12 (median, 11) months after RT, mostly in periods of imaging surveillance. In several patients ($n = 6$), TN first manifested in a late-delayed manner at >5 years, including two cases at 11.9 and 19.9 years, after RT (Fig. 2A).

Radiographically and anatomically, PP predominantly developed around the tumor resection cavity (RC) as a single, nonnodular, ring-like enhancing structure (70.4 vs. 13.5%; $p < .0001$; Fig. 3D–F), whereas TN typically first presented as one or multiple small nodular lesions located at a distance from the RC (Fig. 3A–C) and with greater preference for the periventricular white matter (59.5 vs. 33.3%; $p = .09$; Table 2). Although approximately 60% of patients in both groups developed new ROI-associated neurological symptoms, patients with PP were significantly more likely to receive steroid-based treatment (74.1 vs. 40.5%; $p < .04$) and underwent therapeutic surgical debulking twice as often (51.9 vs. 24.3%). In addition, this group was more likely to receive advanced diagnostic imaging, including MRP and DWI (92.0 vs. 67.6%) to assess radiographically suspicious ROIs, prior to biopsy. Interestingly, in both groups, results from advanced imaging were often suggestive of disease progression rather than treatment-related effects (Table 2). Histopathological analysis of initial ROIs revealed that PP specimens were significantly more likely to contain malignant elements (i.e., treatment effect mixed "with rare atypical cells" or "with foci of solid tumor") than biopsied TN lesions ($p < .04$; Table 2).

Differences in Spatiotemporal Radiographic Lesion Pattern

Longitudinal radiographic evaluation of the 64 PP and TN cases identified a total of 137 individual ROIs ($n = 62$ biopsied; $n = 75$ clinico-radiographic diagnosis). Intergroup

Figure 3. Radiographic evolution of TN and PP over time. T1+ contrast axial magnetic resonance imaging scans from representative patients with TN **(A–C)** and PP **(D–F)** depicting radiographic evolution of treatment-related changes over time. **(A):** Woman aged 37 years with anaplastic oligoastrocytoma status post (s/p) chemoradiation. Onset of biopsy-confirmed TN at 13 months after radiotherapy (RT), presenting as multiple contrast-enhancing lesions (seven total) associated with new neurological symptoms. Gradual regression of lesions under bevacizumab treatment. **(B):** Man aged 64 years with anaplastic astrocytoma s/p RT. At 28 months after RT, onset of multiple periventricularly located, contrast-enhancing lesions (four total) was noted. Follow-up by imaging surveillance showed near total radiographic resolution of all lesions within 1 year of onset without treatment. The dominant left periventricular enhancing lesion is highlighted in the serial scans. **(C):** Woman aged 43 years with anaplastic astrocytoma s/p chemoradiation. Onset of biopsy-confirmed TN at 11 months after chemoradiation (chemo-RT), presenting as multiple contrast-enhancing lesions (nine total) associated with new neurological symptoms, managed with steroids. Eight of nine lesions radiographically resolved within 6 to 26 months of onset. The dominant right periventricular lesion is shown. **(D):** Man aged 39 years with glioblastoma multiforme (GBM) s/p chemoradiation. Increased contrast enhancement around the resection cavity (RC) noted at 3 months after chemo-RT during active antineoplastic treatment. The lesion was associated with new neurological symptoms and was managed with steroids and surgical debulking at 7 months after onset, revealing extensive tissue necrosis. **(E):** Woman aged 65 years with GBM s/p chemoradiation. Increased contrast enhancement around the RC noted at 1 month after chemo-RT during active antineoplastic treatment. The lesion was associated with new neurological symptoms, managed with steroids, partially debulked (4 months after onset), and resolved at 9 months after onset. Histopathology revealed predominant tissue necrosis with few and scattered residual tumor cells. **(F):** Man aged 66 years with GBM s/p chemoradiation. Increased contrast enhancement around the RC noted at 1 month after chemo-RT during active antineoplastic treatment. The lesion was associated with new neurological symptoms, managed with steroids, and fully resected at 4 months after onset, revealing extensive tissue necrosis.
Abbreviations: PP, pseudoprogression; TN, treatment-induced brain tissue necrosis.

Table 3. ROI spatiotemporal radiographic and histopathological characteristics

ROI characteristics	Total cohort	PP group	TN group	*p* value (estimate)[a]
ROI characteristics				
Analyzed ROIs, *n*	137	30	107	
Biopsied, *n*	62	26	36	
Type of biopsy, %				.3580 (−0.7338)
Needle biopsy	40.3	19.2	55.6	
Open resection	53.2	80.8	33.3	
Autopsy	7.7	0.0	11.1	
Not biopsied, but spatiotemporal radiographic pattern similar to a biopsied ROI in same patient, *n*	45	1	44	
Clinico-radiographic diagnosis only, *n*	30	3	27	
Spatiotemporal radiographic features				
Onset after RT completion, median (IQR), months	11 (5–28)	0 (0–2)	16 (10–36)	.0010 (2.4756)
Locations, %				.0001 (−1.4993)
Deep-seated	33.6	6.7	41.1	
Lobar	57.7	73.3	53.3	
Both	8.8	20.0	5.6	
Periventricular location, %	40.2	30.0	43.0	.2600 (0.5651)
Ring-like enhancement around RC, %	18.3	63.3	5.6	<.0001 (−3.3699)
Max. size, median (IQR), cm^2	0.99 (0.16–4.42)	3.70 (1.08–7.50)	0.55 (0.15–3.36)	.1672 (−0.0341)
Shortest distance from RC, median (IQR), mm	16.5 (0.0–27.0)	0.0 (0.0–12.0)	21.5 (10.0–31.0)	.0011 (0.0902)
Correlation to RT dose distribution, %				
Located in main radiation field	98.9 (87/88)	100 (25/25)	98.4 (62/63)	
Radiation dose received, %				
Less than max. therapeutic dose	11.5	8.3	13.0	
Equal to max. therapeutic dose	42.3	29.2	48.1	
More than max. therapeutic dose	46.2	62.5	38.9	
Histopathological features, % (*n*)				.0084 (−1.4779)
Treatment effect only	24.2 (15/62)	0.0 (0/26)	41.7 (15/36)	
Treatment effect with rare atypical cells	56.5 (35/62)	73.1 (19/26)	44.4 (16/36)	
Treatment effect with foci of solid tumor	19.4 (12/62)	26.9 (7/26)	13.9 (5/36)	

[a]Based on a generalized estimating equation model, adjusted for multiple observations per patient, and applied to eight preselected variables of interest.

Abbreviations: IQR, interquartile range; PP, pseudoprogression; RC, resection cavity; ROI, region of interest; RT, radiotherapy; TN, treatment-induced brain tissue necrosis.

comparison at the level of individual ROIs (Table 3) revealed significant differences in both spatial and temporal radiographic lesion pattern. ROIs in the PP group (n = 30) predominantly appeared as unifocal lesions (81.4%), exhibiting a non-nodular, ring-like enhancement pattern at the tumor RC margin with greater frequency than ROIs in patients with TN (63.3 vs. 5.6%; $p < .0001$; Fig. 2C). By contrast, TN-related ROIs (n = 107) were typically nodular, located in deep-seated brain regions ($p = .0001$) at a variable distance from the tumor RC (median, 21.5 mm; range, 0–78 mm; Fig. 2C), and more numerous (median, 2 vs. 1 ROIs; $p = .01$; Table 3). Accordingly, most patients with TN developed multiple nodular ROIs over time (interquartile range, 1–4; max, 12), with approximately one-fourth of ROIs manifesting beyond 3 years after RT completion (Fig. 2B, D).

Whenever possible, individual ROIs were traced longitudinally from time of onset until full radiographic resolution or last available MRI scan (as shown in Fig. 3). For PP-related ROIs, this measurement was mostly precluded as 80% (n = 24/30) of PP lesions were removed surgically and/or treated with antiangiogenics after a median of 4 months after lesion onset. By comparison, only 35% (n = 35/100) of ROIs in the TN group received treatment, after a median of 8 months. The remainder either fully resolved radiographically (36%; median interval, 11.5 months) or persisted until the last available MRI scan (29%; median interval, 15 months).

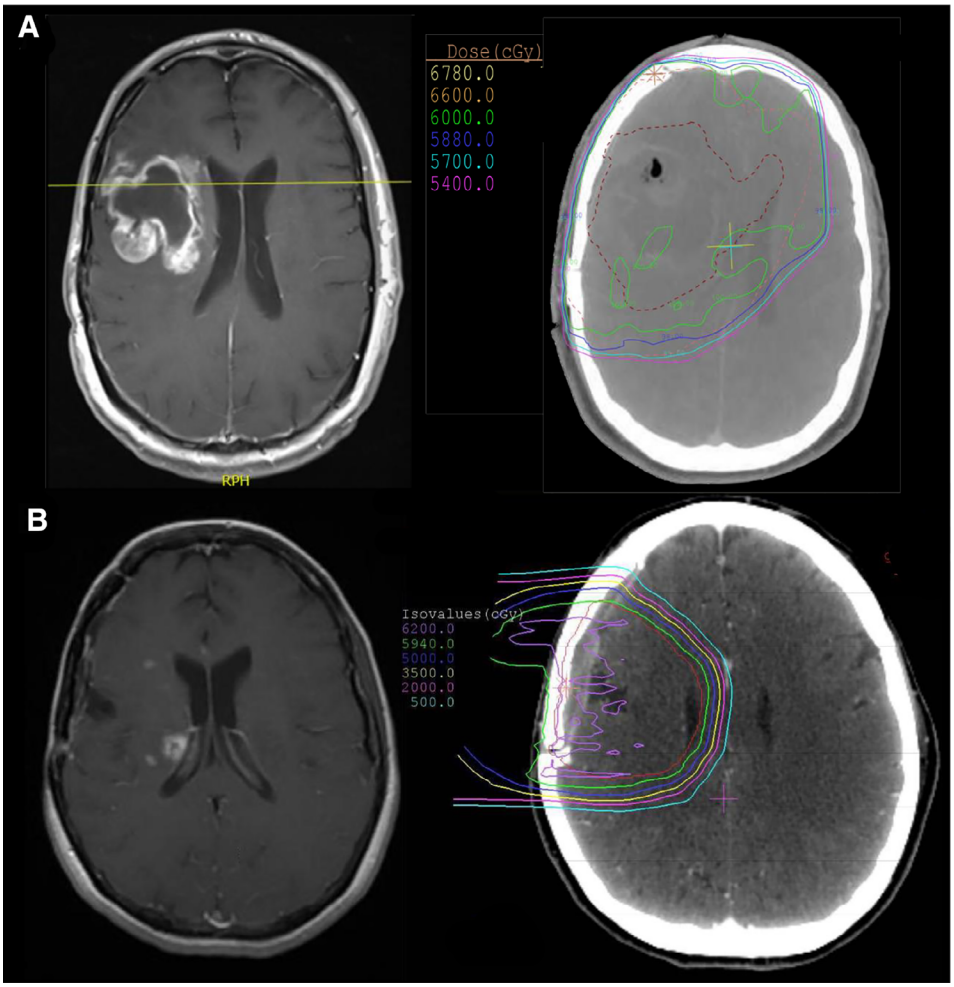

Figure 4. Typical observed radiographic features of treatment-induced brain tissue necrosis (TN) and pseudoprogression (PP). **(A):** Axial T1+ contrast magnetic resonance imaging (MRI) (left) showing a non-nodular focus of enhancement around the tumor resection cavity (RC) in the right frontal lobe, first manifesting at 3 months after radiotherapy (RT), consistent with PP. Corresponding radiotherapy dose distribution overlay on axial computed tomography (right) demonstrates the main radiation field encompassing the RC and surrounding brain parenchyma (60 Gy; green line). **(B):** T1+ contrast MRI (left) showing multiple small nodular foci of enhancement located medially to the RC in the right frontal region with involvement of the periventricular white matter, manifesting at 11 months after RT, consistent with TN. RT dose distribution overlay on axial computed tomography (right) demonstrates prior exposure of these regions of interest to the main radiation field (59.4 Gy; green line).

A correlative analysis between ROI anatomical location and available RT dose distribution curves (as shown in Fig. 4) revealed that 98.9% (n = 87/88) of ROIs were located within the main radiation field, with 46% of ROIs correlating spatially to areas of supratherapeutic radiation maxima (Table 3). Finally, among biopsied ROIs (PP, n = 26; TN, n = 36), TN lesions were found to contain fewer malignant elements (p = .008). Moreover, over one-third of patients with TN underwent a secondary biopsy of the same or a different ROI at a later time point, reconfirming treatment effects.

Discussion

Therapeutic management of patients with brain tumors is frequently complicated by PP and TN. However, diagnostic imaging criteria (including RANO) and clinical guidelines for adequate management remain insufficient. Long-term outcome data represent another area of uncertainty. With this study, we characterize 60 patients with glioma who developed PP or TN as a consequence of brain tumor therapy. Consistent with the clinical literature, we found that treatment-related effects occurred predominantly in patients with HGG after treatment with (TMZ-based) chemo-RT [4, 18, 23]; presented with either early or late radiographic onset (classified here as PP and TN) [2, 15, 16]; were frequently associated with new neurological symptoms [24, 25]; and were treated primarily with steroids, surgical debulking, and/or antiangiogenics [1, 26–28]. Nearly two-thirds of patients had underlying cardiovascular comorbidities, a potential risk factor for treatment-related effects [1]. Presence of either PP or TN appeared to be associated with above-average overall survival.

Comparative analysis by temporal stratification of treatment-related effects suggests that PP and TN are distinct conditions with unique features. Accordingly, we

found that both conditions exhibit significant differences in clinical course and spatiotemporal radiographic pattern and appear to affect distinct patient populations. As such, PP predominantly occurred in patients with GBM, during active antineoplastic treatment in the weeks to few months after chemo-RT, and typically presented on MRI as a unifocal, non-nodular, contrast-enhancing lesion around the RC margin. Affected patients frequently required steroids and surgical debulking and had a worse clinical outcome compared with those with TN. These findings corroborate previous descriptions of PP [4, 14] and support the notion that, rather than merely denoting a radiographic phenomenon, PP should be classified as a distinct clinical condition in neuro-oncology that requires timely diagnosis and appropriate clinical management [2]. Although PP is reportedly enriched in patients with *MGMT* promoter methylated tumors [29, 30], we found that *MGMT* promoter methylation was present in just over half of analyzed tumors in the PP group. Both presence of PP and *MGMT* promoter methylation have been proposed as potential prognostic markers for improved clinical outcome [12, 14, 29, 31, 32]. The observed median OS of 3.25 years in the PP group (81.5% GBM fraction) compares favorably with that historically reported for patients with GBM (approximately 15 months after surgery and chemoradiation) [33], which may support this assumption. Whether and how *IDH1* mutational status affects incidence of PP has been discussed controversially, with some reports suggesting that presence of IHD1 mutation could serve as a possible biomarker for PP [34, 35]. In our cohort, only 11% of patients with PP were found to have *IDH1*-mutated tumors. Our observations are in line with a recent study by Mohammadi et al., who found lower absolute rates of PP expression in patients with GBM with *IDH1*-mutated tumors [36].

Characteristically, TN was enriched in patients with grade III and IV gliomas (mostly *IDH1* mutated and *MGMT* promoter methylated), typically with onset between 7 and 12 months after RT [1], that is, during periods of imaging surveillance. We found that a number of patients presented with either "early necrosis" (n = 2; onset <5 months after RT) [18] or late-delayed TN (n = 6; onset >5 years after RT) [15, 16]. Although the former is most likely a consequence of the increased use of TMZ-based chemo-RT regimens and their radiosensitizing properties [18], the latter may represent a separate form of TN, with distinct pathophysiology, encountered in long-term survivors [1]. Some studies suggest that early TN may predict more durable treatment response and thus potentially improve clinical outcome [18, 21, 37]. We found that the majority of patients with TN were long-term survivors. The comparatively better clinical outcome in this group might be attributed to significant differences in primary diagnosis (GBM fraction 40.5% vs. 81.5%) and incidence rates of tumor *IDH1* mutational status (65 vs. 11%). Moreover, an implicit time bias from including a number of long-term survivors who presented with late-delayed TN is likely a contributing factor, although the vast majority (86%) of TN cases developed relatively early, that is, within 3 years after RT. Although *IDH1* mutation has been identified as an independent positive prognostic biomarker for survival in patients with glioma [38, 39], the relationship between *IDH1* mutational status and development of TN, as with PP, remains understudied. Whether presence of *IDH1* mutation constitutes a direct causal risk factor for TN development or, rather, indirectly increases the probability for TN development by contributing to prolonged OS is unclear.

Radiographically, the manifestation of TN differed from that of PP. TN characteristically presented as multiple small nodular contrast-enhancing lesions, frequently located in the periventricular white matter and/or in other deep-seated brain regions at varying distances from the RC. This corroborates the hypothesis that the delicately vascularized periventricular white matter may serve as a predilection site for TN [4, 6, 37]. Our longitudinal analysis at the level of individual ROIs suggests that some TN lesions persist in a progressive, potentially irreversible manner that may require therapeutic intervention, whereas other lesions are transient and could be sufficiently managed by imaging surveillance. Our findings are in line with recent observations by Van West et al. [37], who analyzed treatment-related effects in patients with low-grade glioma (LGG). In this study, onset of what the authors referred to as "pseudoprogression" occurred in 20% of patients with LGG and after a median of 12 months after RT, presented as asymptomatic, small nodular lesions with frequent location in the ventricle wall, with an average duration of 6 months until radiographic resolution [37]. Concluding that this clinico-radiographic picture differs from what has been described for early pseudoprogression in patients with HGG, the authors reasonably speculated that the observed lesions "could be small areas of radiation necrosis" [37].

Our correlative spatial analysis using RT dose distribution curves revealed that PP and TN lesions almost exclusively developed in the main prior radiation field, that is, those areas previously exposed to therapeutic radiation maxima (42.3%) or supratherapeutic radiation "hot spots" (46.2%). This finding underscores the diagnostic utility of RT dose distribution curves in guiding management of patients with glioma with suspicious, newly enhancing lesions on MRI. It also confirms the central role of RT in the development of treatment-related effects and highlights a clear need for improved protective strategies directed at sparing healthy brain parenchyma from radiation-induced neurotoxicity.

Of note, analysis of TN and PP lesions by MRP and DWI was frequently suggestive of disease progression. Although this finding may highlight the limitations of current advanced imaging modalities in reliably differentiating these conditions from recurrent disease [1, 20], we used a rather conservative binary approach to interpret MRP and DWI imaging reports in this study. Accordingly, evidence of elevated relative cerebral blood volume (or restricted DWI) at individual ROIs—whether mild or substantial—was classified as suggestive of progressive disease. Nonetheless, most patients in our cohort eventually underwent tissue biopsy in order to resolve diagnostic ambiguities on functional imaging. Of note, 25% of biopsy-confirmed PP lesions contained ROIs with "mixed pathology," defined as treatment-related changes with small foci of residual tumor on histopathological analysis [1, 21]. This comparatively higher

incidence of residual malignant elements in PP lesions is likely the result of (a) their direct proximity to the tumor RC margin and (b) their earlier manifestation, that is, during ongoing antineoplastic treatment.

One limitation of this study is that histopathological findings from biopsied lesions were commonly summarized as "treatment effect." Histopathological diagnosis and classification have been limited because of a lack of standardized criteria or guidelines to qualitatively assess and describe different types of treatment-related effects [1]. The distinct clinico-radiographic features of PP and TN strongly suggest that these entities differ in their underlying pathophysiology. For instance, local tissue inflammation and vascular changes produced by surgery-related parenchymal injury could be implicated as plausible mechanisms that drive frequent PP development around the RC margin. Additionally, treatment-induced apoptosis of seeded residual, nonenhancing tumor foci around the RC may fuel the inflammatory environment (with secondary edema and abnormal vessel permeability) thought to contribute to the development of PP [4]. By contrast, the mechanisms driving TN development and their dynamics are likely quite different, as TN lesions mostly occurred during periods of surveillance and in areas previously considered healthy brain parenchyma. The proposed pathological changes implicated in TN—parenchymal necrosis, gliosis, cellular infiltrates, vascular abnormalities, and fibrinous exudates—develop over longer periods of time and are likely more permanent [11]. Robust characterization of putative histopathological differences (e.g., tissue architecture, vascular pathology, cellular inflammatory profile, presence of malignant elements) between PP and TN is warranted and could yield new insights about the pathomechanisms of either condition, with potentially important therapeutic implications.

Our study has several strengths and limitations. Patient selection and data collection were carried out retrospectively, with a focus on patients with glioma with biopsy-confirmed treatment-related effects. Based on the typical manifestation ranges described for both conditions [1, 2, 4, 5, 15, 16], a temporal cutoff point was defined and used as a proxy for patient stratification into PP and TN diagnosis groups. Although we cannot rule out the possibility of diagnostic inaccuracies caused by this strategy, the diagnosis allocated to each patient was carefully reviewed, contextualized with available clinical and radiographic information, and corrected in two instances classified as "early necrosis." Despite the fact that tissue biopsy remains the diagnostic gold standard for PP and TN, there remains a lack of biopsy-confirmed studies in which patients were radiographically diagnosed with treatment-related effects [1]. To our knowledge, our study is the first in which a majority (80%) of cases of treatment-related effects were confirmed by tissue biopsy. Thus, the observed unique characteristics of PP and TN offer insight into their typical clinical course and radiographic spatiotemporal pattern in affected neuro-oncological patients. Moreover, our finding that both conditions preferentially occur in distinct patient populations (i.e., in specific clinical settings) may improve clinician awareness of these distinct conditions and guide patient management. Additionally, our findings suggest that RT dose distribution curves, which correlate with PP and TN, can serve as an important diagnostic tool for the interpretation of suspicious, newly enhancing lesions. Finally, our survival data may support previous studies suggesting that development of treatment-related effects could indicate a more durable treatment response and improved clinical outcome. A comparative analysis with matched controls is warranted to assess whether presence of PP or early TN could indeed serve as an independent positive prognostic biomarker in patients with glioma.

Conclusion

PP and TN appear to occur in clinically distinct patient populations that differ in tumor characteristics, treatment regimen, and clinical outcome. Both conditions exhibit unique features with respect to both clinical course and spatiotemporal radiographic pattern. Use of RT dose distribution curves for delineation of the prior radiation field may serve as an important diagnostic tool to differentiate these conditions from recurrent disease. In line with previous reports, the presence of either PP or TN may be associated with improved overall survival. Increased clinician familiarity with these distinct brain cancer treatment–related conditions and their unique features will improve early detection and diagnosis as well as patient management and thus may circumvent unnecessary surgical procedures.

Acknowledgments

The authors wish to thank Mia S. Bertalan for valuable technical assistance with accessing the Massachusetts General Hospital institutional database used for this study. Portions of this manuscript were presented by S.FW. at the 2018 Society for Neuro-Oncology Scientific Meeting in New Orleans, LA, and the 2019 American Academy of Neurology Annual Meeting in Philadelphia, PA.

Author Contributions

Sebastian F. Winter, Eugene J. Vaios, Alona Muzikansky, Maria Martinez-Lage, Marc R. Bussière, Helen A. Shih, Jay Loeffler, Philipp Karschnia, Franziska Loebel, Peter Vajkoczy, Jorg Dietrich

Conception/design: Sebastian F. Winter, Jorg Dietrich

Provision of study material or patients: Marc R. Bussière, Helen A. Shih, Jay Loeffler, Jorg Dietrich

Collection and/or assembly of data: Sebastian F. Winter

Data analysis and interpretation: Sebastian F. Winter, Eugene J. Vaios, Alona Muzikansky, Maria Martinez-Lage, Marc R. Bussière, Helen A. Shih, Jay Loeffler, Philipp Karschnia, Franziska Loebel, Peter Vajkoczy, Jorg Dietrich

Manuscript writing: Sebastian F. Winter, Eugene J. Vaios, Alona Muzikansky, Maria Martinez-Lage, Marc R. Bussière, Helen A. Shih, Jay Loeffler, Philipp Karschnia, Franziska Loebel, Peter Vajkoczy, Jorg Dietrich

Final approval of manuscript: Sebastian F. Winter, Eugene J. Vaios, Alona Muzikansky, Maria Martinez-Lage, Marc R. Bussière, Helen A. Shih, Jay Loeffler, Philipp Karschnia, Franziska Loebel, Peter Vajkoczy, Jorg Dietrich

Disclosures

The authors indicated no financial relationships.

References

1. Winter SF, Loebel F, Loeffler J et al. Treatment-induced brain tissue necrosis: A clinical challenge in neuro-oncology. Neuro Oncol 2019 [Epub ahead of print].

2. Dietrich J, Winter S, Klein J. Neuroimaging of brain tumors: Pseudoprogression, pseudoresponse, and delayed effects of chemotherapy and radiation. Semin Neurol 2017;37:589–596.

3. Karschnia P, Parsons MW, Dietrich J. Pharmacologic management of cognitive impairment induced by cancer therapy. Lancet Oncol 2019; 20:e92–e102.

4. Brandsma D, Stalpers L, Taal W et al. Clinical features, mechanisms, and management of pseudoprogression in malignant gliomas. Lancet Oncol 2008;9:453–461.

5. Eisele SC, Dietrich J. Cerebral radiation necrosis: Diagnostic challenge and clinical management. Rev Neurol 2015;61:225–232.

6. Kumar AJ, Leeds NE, Fuller GN et al. Malignant gliomas: MR imaging spectrum of radiation therapy- and chemotherapy-induced necrosis of the brain after treatment. Radiology 2000;217: 377–384.

7. Mullins ME, Barest GD, Schaefer PW et al. Radiation necrosis versus glioma recurrence: Conventional MR Imaging clues to diagnosis. AJNR Am J Neuroradiol 2005;26:1967–1972.

8. Dequesada IM, Quisling RG, Yachnis A et al. Can standard magnetic resonance imaging reliably distinguish recurrent tumor from radiation necrosis after radiosurgery for brain metastases? A radiographic-pathological study. Neurosurgery 2008;63:898–904.

9. Ellingson BM, Chung C, Pope WB et al. Pseudoprogression, radionecrosis, inflammation or true tumor progression? Challenges associated with glioblastoma response assessment in an evolving therapeutic landscape. J Neurooncol 2017;134:495–504.

10. Wen PY, Chang SM, Van den Bent MJ et al. Response assessment in neuro-oncology clinical trials. J Clin Oncol 2017;35:2439–2449.

11. Perry A, Schmidt RE. Cancer therapy-associated CNS neuropathology: An update and review of the literature. Acta Neuropathol 2006; 111:197–212.

12. Kucharczyk MJ, Parpia S, Whitton A et al. Evaluation of pseudoprogression in patients with glioblastoma. Neuro-Oncology Pract 2016;4: npw021.

13. Parvez K, Parvez A, Zadeh G. The diagnosis and treatment of pseudoprogression, radiation necrosis and brain tumor recurrence. Int J Mol Sci 2014;15:11832–11846.

14. Taal W, Brandsma D, De Bruin HG et al. Incidence of early pseudo-progression in a cohort of malignant glioma patients treated with chemoirradiation with temozolomide. Cancer 2008;113:405–410.

15. Tofilon PJ, Fike JR. The radioresponse of the central nervous system: A dynamic process. Radiat Res 2000;153:357–370.

16. Giglio P, Gilbert MR. Cerebral radiation necrosis. Neurologist 2003;9:180–188.

17. Kruser TJ, Mehta MP, Robins HI. Pseudoprogression after glioma therapy: A comprehensive review. Expert Rev Neurother 2013; 13:389–403.

18. Chamberlain MC, Glantz MJ, Chalmers L et al. Early necrosis following concurrent Temodar and radiotherapy in patients with glioblastoma. J Neurooncol 2007;82:81–83.

19. Peca C, Pacelli R, Elefante A et al. Early clinical and neuroradiological worsening after radiotherapy and concomitant temozolomide in patients with glioblastoma: Tumour progression or radionecrosis? Clin Neurol Neurosurg 2009; 111:331–334.

20. Verma N, Cowperthwaite MC, Burnett MG et al. Differentiating tumor recurrence from treatment necrosis: A review of neuro-oncologic imaging strategies. Neuro Oncol 2013;15: 515–534.

21. Yang I, Aghi MK. New advances that enable identification of glioblastoma recurrence. Nat Rev Clin Oncol 2009;6:648–657.

22. Jain R, Narang J, Sundgren PM et al. Treatment induced necrosis versus recurrent/progressing brain tumor: Going beyond the boundaries of conventional morphologic imaging. J Neurooncol 2010;100:17–29.

23. Ruben JD, Dally M, Bailey M et al. Cerebral radiation necrosis: Incidence, outcomes, and risk factors with emphasis on radiation parameters and chemotherapy. Int J Radiat Oncol 2006;65: 499–508.

24. Chi D, Béhin A, Delattre JY. Neurologic complications of radiation therapy. In: Schiff D, Kesari S, Wen P et al., eds. Cancer Neurology in Clinical Practice: Neurologic Complications of Cancer and Its Treatment. Totowa, NJ: Humana Press, 2008:259–286.

25. Minniti G, Clarke E, Lanzetta G et al. Stereotactic radiosurgery for brain metastases: analysis of outcome and risk of brain radionecrosis. Radiat Oncol 2011;6:48.

26. Shaw PJ, Bates D. Conservative treatment of delayed cerebral radiation necrosis. J Neurol Neurosurg Psychiatry 1984;47:1338–1341.

27. McPherson CM, Warnick RE. Results of contemporary surgical management of radiation necrosis using frameless stereotaxis and intraoperative magnetic resonance imaging. J Neurooncol 2004;68:41–47.

28. Lubelski D, Abdullah KG, Weil RJ et al. Bevacizumab for radiation necrosis following treatment of high grade glioma: A systematic review of the literature. J Neurooncol 2013;115: 317–322.

29. Brandes AA, Franceschi E, Tosoni A et al. MGMT promoter methylation status can predict the incidence and outcome of pseudoprogression after concomitant radiochemotherapy in newly diagnosed glioblastoma patients. J Clin Oncol 2008;26:2192–2197.

30. Yoon RG, Kim HS, Paik W et al. Different diagnostic values of imaging parameters to predict pseudoprogression in glioblastoma subgroups stratified by MGMT promoter methylation. Eur Radiol 2017;27:255–266.

31. Dworkin M, Mehan W, Niemierko A et al. Increase of pseudoprogression and other treatment related effects in low-grade glioma patients treated with proton radiation and temozolomide. J Neurooncol 2019;142:69–77.

32. Gerstner ER, McNamara MB, Norden AD et al. Effect of adding temozolomide to radiation therapy on the incidence of pseudo-progression. J Neurooncol 2009;94:97–101.

33. Stupp R, Mason WP, van den Bent MJ et al. Radiotherapy plus concomitant and adjuvant temozolomide for glioblastoma. N Engl J Med 2005;352:987–996.

34. Motegi H, Kamoshima Y, Terasaka S et al. IDH1 mutation as a potential novel biomarker for distinguishing pseudoprogression from true progression in patients with glioblastoma treated with temozolomide and radiotherapy. Brain Tumor Pathol 2013;30:67–72.

35. Li H, Li J, Cheng G et al. IDH mutation and MGMT promoter methylation are associated with the pseudoprogression and improved prognosis of glioblastoma multiforme patients who have undergone concurrent and adjuvant temozolomide-based chemoradiotherapy. Clin Neurol Neurosurg 2016;151:31–36.

36. Mohammadi H, Shiue K, Grass GD et al. Isocitrate dehydrogenase 1 mutant glioblastomas demonstrate a decreased rate of pseudoprogression: A multi-institutional experience. Neurooncol Pract 2019;7:185–195.

37. van West SE, de Bruin HG, van de Langerijt B et al. Incidence of pseudoprogression in low-grade gliomas treated with radiotherapy. Neuro Oncol 2017;19:719–725.

38. Nobusawa S, Watanabe T, Kleihues P et al. IDH1 mutations as molecular signature and predictive factor of secondary glioblastomas. Clin Cancer Res 2009;15:6002–6007.

39. Sanson M, Marie Y, Paris S et al. Isocitrate dehydrogenase 1 codon 132 mutation is an important prognostic biomarker in gliomas. J Clin Oncol 2009;27:4150–4154.